Analytical parametrization of fusion barriers using proximity potentials

Ishwar Dutt and Rajeev K. Puri*
Department of Physics, Panjab University, Chandigarh 160014, India
(Received 1 April 2010; published 21 June 2010)

Using the three versions of proximity potentials, namely proximity 1977, proximity 1988, and proximity 2000, we present a pocket formula for fusion barrier heights and positions. This was achieved by analyzing as many as 400 reactions with mass between 15 and 296. Our parametrized formula can reproduced the exact barrier heights and positions within an accuracy of ±1%. A comparison with the experimental data is also in good agreement.

DOI: 10.1103/PhysRevC.81.064608 PACS number(s): 25.70.Jj, 24.10.−i

I. INTRODUCTION

In the low energy heavy-ion collisions, fusion of colliding nuclei and related phenomena has always been of central interest [1]. Depending upon the incident energy of the projectile as well as angular momentum and impact parameter, the collision of nuclei can lead to several interesting phenomena such as incomplete fusion [1], multifragmentation [2,3], subthreshold particle production [4], nuclear flow [5] as well as formation of the superheavy elements [6]. Since fusion is a low density phenomenon, several mean field models [1,6–11] have been developed in the recent past at microscopic/macroscopic level and have been robust against the vast experimental data [10–12] that range from symmetric to highly asymmetric colliding nuclei. The study of mass dependence has always guided the validity of various models irrespective of the energy range. The essential idea of developing a model is to understand the physical mechanism behind a process or phenomenon. Extension of the physics is also reported toward isospin degree of freedom. At the same time, accumulation of huge experimental data [10–12] (that include all kinds of masses and asymmetry of colliding nuclei) puts stringent test for any theoretical model.

As fusion process occurs at the surface of colliding nuclei, any difference occurring in the interior part of the potential does not make any difference toward the fusion. One always tries to parametrize the potential in terms of some known quantities such as the masses and charges of colliding nuclei [1,9,13,14]. At intermediate energies, several forms of density dependent potentials are also available [2–5]. Generally, the benchmark is to parameterized the outcome in proximity fashion [7]. By adding the Coulomb potential to the parameterized form of the nuclear ion-ion potential, one obtains total ion-ion potential and ultimately, the fusion barriers and cross sections.

Alternatively, one calculates the barrier heights as well as positions of large number of reactions and then tries to parametrize these in terms of some known quantities like the charges and masses of the colliding nuclei [1,15]. Recently, even neutron excess dependence has also been incorporated in some attempts [16]. Similarly, an analytical expression to determine the barrier heights and positions are also presented in Ref. [17]. The cost of such attempts was in the form of more complicated parameterized form. The utility of such direct parametrization is that one can use these pocket formula to find out the fusion barriers instantaneously.

As is evident from the literature, several modifications over the original proximity potential have also been suggested in the recent years [8,10]. We shall here attempt to present a direct parametrization of the fusion barrier positions as well as heights using different proximity potentials. This attempt will introduce great simplification in obtaining the fusion barrier positions and heights. Section II describes the models in brief, Sec. III depicts the results, and a summary is presented in Sec. IV.

II. THE MODEL

All proximity potentials are based on the proximity force theorem. According to which, *"the force between two gently curved surfaces in close proximity is proportional to the interaction potential per unit area between the two flat surfaces"*. The nuclear part of the interaction potential in different proximity potentials is described as a product of geometrical factor representing the mean curvature of the interacting surfaces and an universal function depending on the separation distance.

A. Proximity 1977 (Prox 77)

According to the original version of proximity [7], the interaction potential $V_N(r)$ between two surfaces can be written as

$$V_N^{\text{Prox77}}(r) = 4\pi\gamma b\overline{R}\Phi\left(\frac{r - C_1 - C_2}{b}\right)\text{MeV}, \qquad (1)$$

where the surface energy coefficient γ taken from the Lysekil mass formula (in MeV/fm^2) is written as

$$\gamma = \gamma_0[1 - k_s I^2], \qquad (2)$$

with $I = (\frac{N-Z}{A})$; N, Z, and A refer to the neutron, proton and total mass of two interacting nuclei. Though the proximity potential Prox 77, in principle, is for zero-neutron excess, the factor γ takes care of some neutron excess content. In the above formula, γ_0 is the surface energy constant and k_s is the surface-asymmetry constant. Both constants were first parametrized by

*rkpuri@pu.ac.in; drrkpuri@gmail.com

Myers and Świątecki [18] by fitting the experimental binding energies. The first set of these constants yielded values γ_0 and $k_s = 1.017\,34$ MeV/fm^2 and 1.79, respectively. Later on, these values were revised to $\gamma_0 = 0.951\,7$ MeV/fm^2 and $k_s = 1.782\,6$ [19]. Interestingly, most of the modified proximity type potentials use different values of the parameter γ [8,10]. The mean curvature radius, $\overline{R}$ in Eq. (1) has the form

$$\overline{R} = \frac{C_1 C_2}{C_1 + C_2}, \tag{3}$$

quite similar to the one used for reduced mass. Here

$$C_i = R_i \left[1 - \left(\frac{b}{R_i} \right)^2 + \cdots\cdots \right], \tag{4}$$

R_i, the effective sharp radius, reads as

$$R_i = 1.28\, A_i^{1/3} - 0.76 + 0.8\, A_i^{-1/3}\ \text{fm} \quad (i = 1, 2). \tag{5}$$

The universal function $\Phi(\xi)$ was parametrized with the following form:

$$\Phi(\xi) = \begin{cases} -\frac{1}{2}(\xi - 2.54)^2 - 0.0852(\xi - 2.54)^3, \\ \text{for } \xi \leqslant 1.2511, \\ -3.437 \exp\left(-\frac{\xi}{0.75}\right), \\ \text{for } \xi \geqslant 1.2511, \end{cases} \tag{6}$$

with $\xi = (r - C_1 - C_2)/b$. The width b has been evaluated close to unity. Using the above form, one can calculate the nuclear part of the interaction potential $V_N(r)$. This model is referred as Prox 77 and corresponding potential as $V_N^{\text{Prox77}}(r)$.

B. Proximity 1988 (Prox 88)

Later on, using the more refined mass formula of Möller and Nix [20], the value of coefficients γ_0 and k_s were modified yielding their values 1.249 6 MeV/fm^2 and 2.3, respectively. Reisdorf [8] labeled this modified version as 'Proximity 1988'. Note that this set of coefficients give stronger attraction compared to the above sets. Even a more recent compilation by Möller and Nix [21] yields similar values. We marked this potential as Prox 88.

C. Proximity 2000 (Prox 00)

Recently, Myers and Świątecki [10] modified Eq. (1) by using up-to-date knowledge of nuclear radii and surface tension coefficients using their droplet model concept. The prime aim behind this attempt was to remove discrepancy of the order of 4% reported between the results of Prox 77 and experimental data [10]. Using the droplet model [22], matter radius C_i was calculated as

$$C_i = c_i + \frac{N_i}{A_i} t_i \quad (i = 1, 2), \tag{7}$$

where c_i denotes the half-density radii of the charge distribution and t_i is the neutron skin of the nucleus. To calculate c_i, these authors [10] used two-parameter Fermi function values given in Ref. [23] and remaining cases were handled with the help of parametrization of charge distribution described below.

The nuclear charge radius (denoted as R_{00} in Ref. [24]) is given by the relation:

$$R_{00i} = \sqrt{\frac{5}{3}} \langle r^2 \rangle^{1/2} = 1.240 A_i^{1/3} \left\{ 1 + \frac{1.646}{A_i} - 0.191 \times \left(\frac{A_i - 2Z_i}{A_i} \right) \right\} \text{ fm} \quad (i = 1, 2), \tag{8}$$

where $\langle r^2 \rangle$ represents the mean square nuclear charge radius. According to Ref. [24], Eq. (8) was valid for the even-even nuclei with $8 \leqslant Z < 38$ only. For nuclei with $Z \geqslant 38$, the above equation was modified by Pomorski *et al.* [24] as

$$R_{00i} = 1.256 A_i^{1/3} \left\{ 1 - 0.202 \left(\frac{A_i - 2Z_i}{A_i} \right) \right\} \text{fm}. \tag{9}$$

These expressions give good estimate of the measured mean square nuclear charge radius $\langle r^2 \rangle$. In the present model, authors used only Eq. (8). The half-density radius, c_i was obtained from the relation:

$$c_i = R_{00i} \left(1 - \frac{7}{2} \frac{b^2}{R_{00i}^2} - \frac{49}{8} \frac{b^4}{R_{00i}^4} + \cdots \right) \quad (i = 1, 2). \tag{10}$$

Using the droplet model [22], neutron skin t_i reads as

$$t_i = \frac{3}{2} r_0 \left[\frac{J I_i - \frac{1}{12} c_1 Z_i A_i^{-1/3}}{Q + \frac{9}{4} J A_i^{-1/3}} \right] \quad (i = 1, 2). \tag{11}$$

Here r_0 is 1.14 fm, the value of nuclear symmetric energy coefficient $J = 32.65$ MeV and $c_1 = 3e^2/5r_0 = 0.757\,895$ MeV. The neutron skin stiffness coefficient Q was taken to be 35.4 MeV. The nuclear surface energy coefficient γ in terms of neutron skin was given as

$$\gamma = \frac{1}{4\pi r_0^2} \left[18.63\,(\text{MeV}) - Q \frac{(t_1^2 + t_2^2)}{2r_0^2} \right], \tag{12}$$

where t_1 and t_2 were calculated using Eq. (11). The universal function $\Phi(\xi)$ is reported as

$$\Phi(\xi) = \begin{cases} -0.135\,3 + \sum_{n=0}^{5} [c_n/(n+1)](2.5 - \xi)^{n+1}, \\ \text{for } 0 < \xi \leqslant 2.5, \\ -0.095\,51 \exp[(2.75 - \xi)/0.717\,6], \\ \text{for } \xi \geqslant 2.5. \end{cases} \tag{13}$$

The values of different constants c_n were: $c_0 = -0.188\,6$, $c_1 = -0.262\,8$, $c_2 = -0.152\,16$, $c_3 = -0.045\,62$, $c_4 = 0.069\,136$, and $c_5 = -0.011\,454$. For $\xi > 2.74$, the above exponential expression is the exact representation of the Thomas-Fermi extension of the proximity potential. This potential is marked as Prox 00.

III. RESULTS AND DISCUSSION

As a first step, we calculated the nuclear part of the ion-ion potential using Prox 77, Prox 88, and Prox 00 potentials and

then by adding the Coulomb potential ($=\frac{Z_1 Z_2 e^2}{r}$), total ion-ion potential $V_T(r)$ for spherical colliding pair is obtained. The fusion barrier is then extracted using conditions

$$\left.\frac{dV_T(r)}{dr}\right|_{r=R_B} = 0, \quad \text{and} \quad \left.\frac{d^2V_T(r)}{dr^2}\right|_{r=R_B} \leqslant 0. \qquad (14)$$

The height of the barrier and position is marked, respectively, as V_B and R_B. For the present analysis, all kind of the reactions involving symmetric ($N = Z, A_1 = A_2$) as well as asymmetric ($N \neq Z, A_1 \neq A_2$) nuclei are considered. In all, 400 reactions covering almost whole of the periodic table are taken into account. All nuclei considered here are assumed to be spherical in nature, however, deformation as well as orientation of the nuclei also affect the fusion barriers [25]. The lightest reaction considered here is ^{6}Li + ^{9}Be whereas the heaviest one is ^{48}Ca + ^{248}Cm. As reported in Ref. [10], proximity Prox 77 overestimate experimental data by 4%. It was reported to be better for newer versions.

Once fusion barrier heights and positions were calculated, a search was made for their parametrization. Since it is evident that barrier positions depend on the size of the colliding systems, the best way is to parametrize them in terms of the radius dependence i.e. in terms of $A^{1/3}$. In the literature, several attempts exist that parametrize R_B directly either as $A' + B'(A_1^{1/3} + A_2^{1/3})$ [26–29] or as $r_B(=\frac{R_B}{A_1^{1/3}+A_2^{1/3}})$ [30,31]. We have also tried similar fits. Unfortunately, the scattering around the mean curve was quite significant in both the cases, therefore, we discard this kind of parametrizations. Alternatively, we plotted the reduced fusion barrier positions $s_B = R_B - C_1 - C_2$, as a function of $\frac{Z_1 Z_2}{A_1^{1/3}+A_2^{1/3}}$ for all three versions of proximity potentials (see Fig. 1). Very encouragingly, the reduced barrier positions s_B of all the reactions fall on the mean curve that can be parameterized in terms of exponential function. We noted that the scattering around the mean positions is very small. Due to the weak Coulomb force in lighter colliding nuclei, lesser attractive potential is needed to counterbalance it. As a result, separation distance increases in lighter colliding nuclei. As we go to heavier nuclei, stronger Coulomb contribution demands more and more penetration, therefore, decreasing the value of s_B. In other words, the fusion in lighter nuclei occurs at the outer region compared to the heavier nuclei where s_B is much smaller.

If we compare (a) and (b) parts of the Fig. 1, we notice that s_B, the separation distance between nuclei is slightly more in Prox 88 compared to Prox 77. This is due to the fact that Prox 88 has stronger surface energy coefficient γ [see Eq. (2) with $\gamma_0 = 1.249\,6$ MeV/fm^2 and $k_s = 2.3$, respectively]. This results in more attractive nuclear potential compared to Prox 77 and therefore, counterbalancing happens at larger distances. From the figure, it is also evident that latest proximity potential has shallow nuclear potential compared to the other two versions. All three proximity potentials follow similar mass/charge dependence and can be parametrized in terms of following function:

$$s_B^{\text{par}} = \alpha \exp[-\beta(x-2)^{1/4}]. \qquad (15)$$

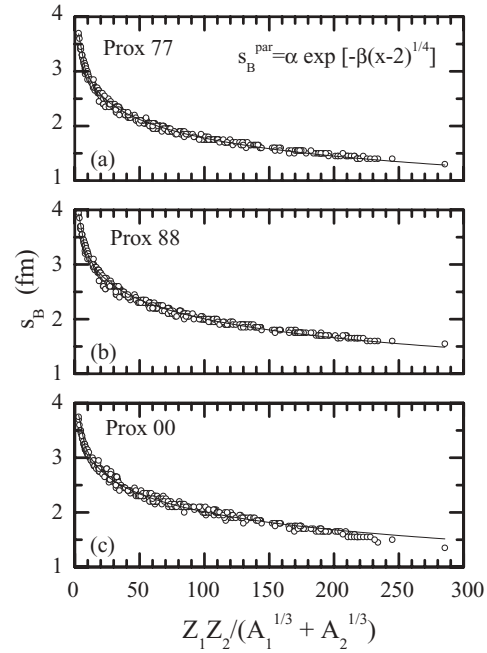

FIG. 1. Reduced fusion barrier positions s_B (fm) (defined as $s_B = R_B - C_1 - C_2$) as a function of the $\frac{Z_1 Z_2}{A_1^{1/3}+A_2^{1/3}}$. Parts (a), (b), and (c) show the results with Prox 77, Prox 88, and Prox 00 versions of the proximity potential. Our parametrized fits are shown as solid curves. The values of constants α and β are given in the text.

Here, $x = \frac{Z_1 Z_2}{A_1^{1/3}+A_2^{1/3}}$ and α, β are the constants whose values depend on the model one is using. The values of α, are 5.184 19, 5.374 57, and 5.087 58, whereas the values of β are 0.339 79, 0.313 26, and 0.295 18 for Prox 77, Prox 88, and Prox 00, potentials, respectively. The analytical parametrized fusion barrier positions therefore, read as

$$R_B^{\text{par}} = s_B^{\text{par}} + C_1 + C_2. \qquad (16)$$

The quality of our parametrized fusion positions can be judged by analyzing the percentage deviation defined as

$$\Delta R_B(\%) = \frac{R_B^{\text{par}} - R_B^{\text{exact}}}{R_B^{\text{exact}}} \times 100. \qquad (17)$$

We plot in Fig. 2, the percentage deviation $\Delta R_B(\%)$ as a function of the product of charges $Z_1 Z_2$. Very encouragingly, we see that in all three cases, our analytical parametrized form gives very good results within $\pm 1\%$ of the actual exact barriers positions. The average deviations calculated over 400 reactions are -0.01%, -0.02%, and 0% for Prox 77, Prox 88, and Prox 00, respectively. This is very encouraging since it is for the first time that such accurate parametrization has been obtained. Note that our parametrizations depend on the charges and masses of the colliding nuclei only. This definitely introduces great simplification in the calculation of fusion barrier positions within proximity concept.

In Fig. 3, we parametrize the fusion barrier heights V_B as a function of $\frac{1.44 Z_1 Z_2}{R_B^{\text{par}}}(1 - \frac{0.75}{R_B^{\text{par}}})$, similar to the one reported in Refs. [16,27]. The first part is the Coulomb contribution

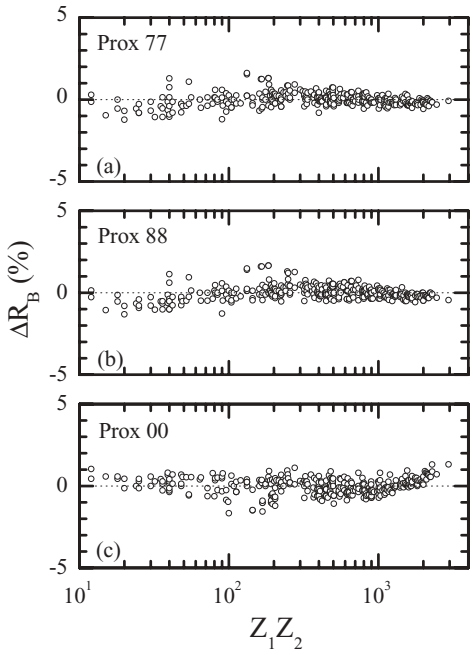

FIG. 2. The percentage difference $\Delta R_B(\%)$ [defined in Eq. (17)] as a function of the product of charges of colliding pair Z_1Z_2. Parts (a), (b), and (c) show the results with Prox 77, Prox 88, and Prox 00 versions of the proximity potential.

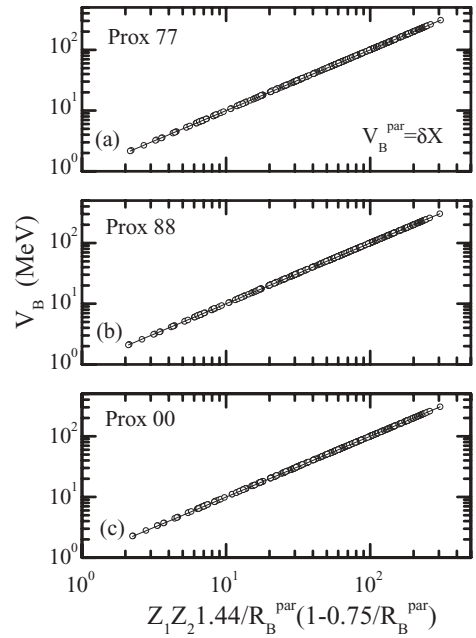

FIG. 3. The fusion barrier heights V_B (MeV), as a function of $\frac{1.44Z_1Z_2}{R_B^{\rm par}}(1-\frac{0.75}{R_B^{\rm par}})$. Parts (a), (b), and (c) show the results with Prox 77, Prox 88, and Prox 00 versions of the proximity potential. Our parametrized fits are shown as solid curves. The value of the constant δ is given in the text.

whereas the second part is the reduction due to the nuclear potential. We see that the fusion barrier heights in all three proximity potentials can be parametrized using the following relation:

$$V_B^{\rm par} = \delta\left[\frac{1.44Z_1Z_2}{R_B^{\rm par}}\left(1-\frac{0.75}{R_B^{\rm par}}\right)\right]. \qquad (18)$$

Where δ is a constant having values 0.999 03, 0.998 68, and 1.002 for Prox 77, Prox 88, and Prox 00, respectively. Here second term in the above relation is introduced to take care of the deviations that happen in the lower tail of the fusion barrier heights. We see that one can parametrize the barrier heights very closely. The quality of our analytical parametrization is tested in Fig. 4, where again percentage difference between parametrized and exact values are shown. Mathematically,

$$\Delta V_B(\%) = \frac{V_B^{\rm par} - V_B^{\rm exact}}{V_B^{\rm exact}} \times 100. \qquad (19)$$

Very encouragingly, we see that our fits are within $\pm 1\%$ of the actual values. Some slight deviations can be seen for lighter masses. This may also be due to the limitations of proximity potentials in handling the lighter masses where surface is of the order of nuclear radius. It is very encouraging to note that our parametrized form give barrier heights and positions within $\pm 1\%$ of the actual values. The average deviations are -0.10%, -0.12%, and 0.07% for Prox 77, Prox 88, and Prox 00, respectively. In Table I, we display the actual and analytical parametrized values of some selected collisions for all three versions of proximity potentials. We note that our results are in very close agreement with the actual value and therefore, introduces great simplification in the calculation of fusion barriers. Finally, we compare our outcome with experimental data in Fig. 5. Here we display our analytically parametrized fusion barrier heights $V_B^{\rm par}$ [Eq. (19)] with experimentally extracted fusion barrier heights $V_B^{\rm expt}$.

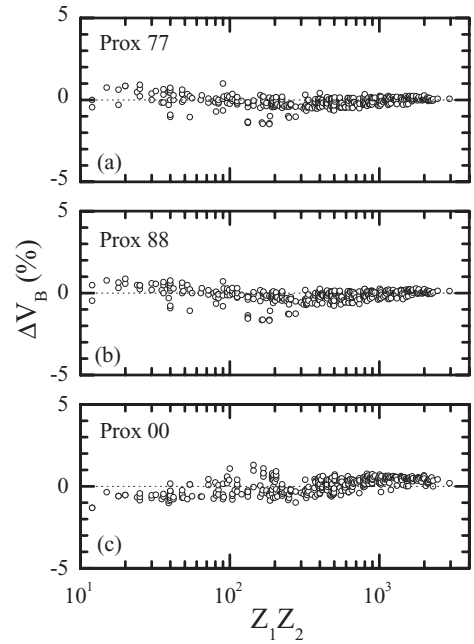

FIG. 4. Same as Fig. 2, but for $\Delta V_B(\%)$.

TABLE I. Fusion barrier heights V_B (in MeV) and positions R_B (in fm), calculated using different proximity potentials along with their corresponding parametrized values are displayed for few cases.

Reaction	Prox 77		Prox 88		Prox 00		Prox 77		Prox 88		Prox 00	
	R_B^{exact}	R_B^{par}	R_B^{exact}	R_B^{par}	R_B^{exact}	R_B^{par}	V_B^{exact}	V_B^{par}	V_B^{exact}	V_B^{par}	V_B^{exact}	V_B^{par}
^{6}Li + ^{9}Be	7.01	7.03	7.26	7.27	6.74	6.81	2.21	2.20	2.14	2.13	2.29	2.26
^{10}B + ^{12}C	7.22	7.21	7.47	7.45	6.99	7.03	5.36	5.36	5.19	5.20	5.54	5.50
^{16}O + ^{16}O	7.65	7.65	7.90	7.90	7.51	7.54	10.86	10.86	10.55	10.55	11.10	11.03
^{20}Ne + ^{20}Ne	7.95	7.97	8.20	8.21	8.42	8.28	16.39	16.35	15.94	15.92	15.68	15.85
^{24}Mg + ^{26}Mg	8.40	8.37	8.65	8.61	8.86	8.73	22.54	22.53	21.95	21.96	21.47	21.75
^{24}Mg + ^{34}S	8.61	8.61	8.86	8.85	8.89	8.80	29.34	29.28	28.60	28.55	28.64	28.80
^{16}O + ^{64}Ni	9.01	9.03	9.26	9.27	9.05	9.08	35.17	35.06	34.33	34.22	35.08	34.99
^{6}Li + ^{238}U	10.87	10.97	11.07	11.21	10.81	10.93	34.07	33.72	33.46	33.04	34.28	33.94
^{12}C + ^{124}Sn	9.88	9.94	10.13	10.18	9.97	10.00	40.31	40.14	39.49	39.26	40.20	40.04
^{16}O + ^{110}Pd	9.88	9.90	10.08	10.13	10.02	10.01	49.60	49.42	48.56	48.38	49.12	49.07
^{30}Si + ^{64}Ni	9.63	9.60	9.83	9.84	9.71	9.65	54.13	54.16	52.94	52.92	53.93	54.06
^{48}Ca + ^{48}Ca	9.89	9.81	10.09	10.05	9.89	9.83	53.96	54.18	52.84	52.97	53.93	54.24
^{32}S + ^{58}Ni	9.40	9.45	9.65	9.68	9.50	9.53	63.04	62.79	61.60	61.40	62.64	62.49
^{40}Ar + ^{60}Ni	9.82	9.78	10.02	10.02	10.00	9.94	68.40	68.45	66.91	66.92	67.37	67.64
^{16}O + ^{166}Er	10.64	10.66	10.84	10.89	10.77	10.76	68.56	68.25	67.25	66.89	67.93	67.87
^{16}O + ^{186}W	10.86	10.90	11.06	11.13	11.18	11.15	73.09	72.76	71.74	71.34	71.39	71.45
^{36}S + ^{90}Zr	10.30	10.28	10.55	10.50	10.41	10.36	82.99	83.03	81.30	81.39	82.35	82.69
^{35}Cl + ^{92}Zr	10.25	10.25	10.50	10.47	10.39	10.36	88.58	88.45	86.75	86.71	87.64	87.85
^{32}S + ^{110}Pd	10.43	10.45	10.68	10.68	10.65	10.65	94.21	94.05	92.33	92.15	92.43	92.70
^{64}Ni + ^{64}Ni	10.48	10.47	10.73	10.70	10.60	10.57	99.84	100.00	97.86	97.98	98.90	99.43
^{40}Ar + ^{110}Pd	10.75	10.73	10.95	10.95	11.07	10.98	103.19	103.25	101.21	101.30	100.61	101.37
^{32}S + ^{138}Ba	10.87	10.87	11.07	11.09	10.93	10.96	110.71	110.40	108.62	108.33	109.73	109.89
^{40}Ar + ^{130}Te	11.05	11.03	11.25	11.26	11.22	11.18	113.63	113.78	111.56	111.58	111.96	112.69
^{24}Mg + ^{208}Pb	11.41	11.44	11.61	11.66	11.73	11.69	116.04	115.63	114.02	113.56	113.09	113.66
^{29}Si + ^{178}Hf	11.27	11.28	11.47	11.50	11.55	11.49	120.24	120.00	118.08	117.83	117.75	118.32
^{34}S + ^{168}Er	11.35	11.32	11.55	11.55	11.39	11.40	129.16	129.10	126.86	126.67	128.04	128.65
^{64}Ni + ^{96}Zr	11.13	11.08	11.33	11.30	11.21	11.19	135.37	135.58	132.87	133.07	134.04	134.74
^{38}S + ^{181}Ta	11.69	11.64	11.89	11.87	11.79	11.78	134.80	135.05	132.51	132.56	133.21	133.96
^{48}Ca + ^{154}Sm	11.61	11.59	11.86	11.80	11.72	11.68	143.72	143.95	141.26	141.51	142.55	143.35
^{40}Ar + ^{180}Hf	11.65	11.66	11.90	11.88	11.81	11.80	149.63	149.61	147.07	146.98	147.58	148.40
^{38}S + ^{208}Pb	11.98	11.94	12.18	12.16	12.00	12.00	147.89	148.15	145.47	145.60	147.31	147.90
^{64}Ni + ^{124}Sn	11.55	11.52	11.75	11.73	11.68	11.68	163.23	163.45	160.37	160.67	160.85	161.84
^{40}Ar + ^{206}Pb	11.93	11.94	12.18	12.16	12.11	12.10	166.66	166.67	163.89	163.79	164.19	165.10
^{86}Kr + ^{100}Mo	11.59	11.57	11.84	11.79	11.68	11.70	175.40	175.81	172.33	172.69	173.67	174.51
^{90}Zr + ^{90}Zr	11.42	11.42	11.67	11.64	11.56	11.59	188.23	188.32	184.79	184.94	185.53	186.30
^{40}Ar + ^{238}U	12.31	12.28	12.51	12.49	12.30	12.35	182.29	182.15	179.41	179.22	181.07	181.72
^{96}Mo + ^{100}Mo	11.75	11.72	11.95	11.93	11.81	11.86	202.39	202.67	198.85	199.28	200.05	201.03
^{54}Cr + ^{196}Os	12.22	12.19	12.42	12.40	12.34	12.34	201.86	202.01	198.62	198.75	199.21	200.31
^{51}V + ^{208}Pb	12.23	12.24	12.48	12.45	12.36	12.40	208.11	208.09	204.75	204.73	205.18	206.18
^{54}Cr + ^{209}Bi	12.33	12.32	12.53	12.53	12.59	12.61	218.37	218.45	214.85	214.95	212.95	214.38
^{96}Zr + ^{124}Sn	12.15	12.13	12.40	12.34	12.28	12.29	222.18	222.53	218.53	218.91	219.15	220.48
^{55}Mn + ^{208}Pb	12.35	12.32	12.55	12.53	12.24	12.35	224.74	224.80	221.13	221.20	224.89	224.96
^{70}Zn + ^{176}Yb	12.35	12.31	12.55	12.52	12.36	12.41	230.12	230.47	226.42	226.76	228.67	229.41
^{58}Fe + ^{208}Pb	12.39	12.40	12.64	12.61	12.38	12.47	232.38	232.38	228.67	228.68	231.26	231.85
^{59}Co + ^{208}Pb	12.42	12.41	12.62	12.62	12.50	12.57	241.20	241.15	237.34	237.30	237.99	238.98
^{59}Co + ^{209}Bi	12.43	12.42	12.63	12.63	12.62	12.69	244.02	243.90	240.10	240.01	238.47	239.75
^{63}Cu + ^{197}Au	12.39	12.37	12.59	12.57	12.20	12.36	250.40	250.29	246.33	246.46	251.22	251.22
^{64}Ni + ^{208}Pb	12.56	12.54	12.76	12.75	12.53	12.64	247.56	247.65	243.66	243.74	245.68	246.54
^{70}Zn + ^{208}Pb	12.71	12.67	12.91	12.87	12.76	12.85	262.60	262.78	258.53	258.86	259.01	260.10
^{86}Kr + ^{208}Pb	12.99	12.98	13.24	13.18	12.92	13.09	308.05	308.27	303.40	303.77	306.16	306.75

The experimentally extracted fusion barrier heights displayed in this figure are obtained in the approach, when shapes of both colliding nuclei are spherical. The experimental data are taken from Refs [10–12]. It is clear from the figure that our results are in good agreement with experimental data. In a recent attempt [32], we presented comparison of 16 different

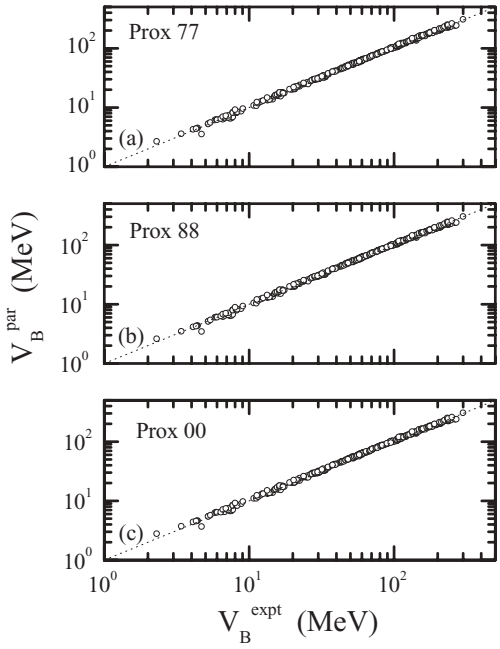

FIG. 5. The variation of the parametrized fusion barrier heights V_B^{par}(MeV) as a function of experimental fusion barrier heights V_B^{expt}(MeV). Parts (a), (b), and (c) show the results with Prox 77, Prox 88, and Prox 00 versions of the proximity potential. The experimental values are taken from Refs. [10–12].

proximity based potentials and found that potentials due to Bass [8], Aage Winther [33], and Denisov [32] (marked as Bass 80, AW 95, and Denisov DP in Ref. [32]) were performing better than other proximity based potentials. The analytical parametrizations of such potentials will be presented elsewhere [34].

IV. SUMMARY

Using three versions of proximity potentials, we obtained analytical relations for the fusion barrier heights and positions. Our analysis is based on the calculations of 400 reactions. Our analytical parameterized values are in very close agreement with actual as well as experimental values. Therefore, introducing great simplifications in the calculation of fusion barrier heights and positions. These results can be used as a guide line for estimating the fusion barriers in those cases where measurements do not exist and also for the study of new nuclei yet unexplored.

ACKNOWLEDGMENTS

This work was supported by a research grant from the Department of Atomic Energy, Government of India.

[1] R. K. Puri *et al.*, Eur. Phys. J. A **23**, 429 (2005); R. Arora *et al.*, *ibid.* **8**, 103 (2000); R. K. Puri *et al.*, *ibid.* **3**, 277 (1998); R. K. Puri, P. Chattopadhyay, and R. K. Gupta, Phys. Rev. C **43**, 315 (1991); R. K. Puri and R. K. Gupta, *ibid.* **45**, 1837 (1992).

[2] Y. K. Vermani, S. Goyal, and R. K. Puri, Phys. Rev. C **79**, 064613 (2009); A. D. Sood and R. K. Puri, *ibid.* **70**, 034611 (2004); J. Singh, S. Kumar, and R. K. Puri, *ibid.* **62**, 044617 (2000); C. Fuchs *et al.*, J. Phys. G: Nucl. Part. Phys. **22**, 131 (1996).

[3] R. K. Puri, C. Hartnack, and J. Aichelin, Phys. Rev. C **54**, R28 (1996); Nucl. Phys. A **575**, 733 (1994); S. Kumar, M. K. Sharma, R. K. Puri, K. P. Singh, and I. M. Govil, Phys. Rev. C **58**, 3494 (1998); R. K. Puri *et al.*, J. Comput. Phys. **162**, 245 (2000); S. Kumar, R. K. Puri, and J. Aichelin, Phys. Rev. C **58**, 1618 (1998).

[4] G. Batko *et al.*, J. Phys. G: Nucl. Part. Phys. **20**, 461 (1994); S. W. Huang *et al.*, Phys. Lett. B **298**, 41 (1993); Prog. Part. Nucl. Phys. **30**, 105 (1993).

[5] E. Lehmann, R. K. Puri, A. Faessler, G. Batko, and S. W. Huang, Phys. Rev. C **51**, 2113 (1995); Prog. Part. Nucl. Phys. **30**, 219 (1993).

[6] R. K. Gupta, S. Singh, R. K. Puri, and W. Scheid, Phys. Rev. C **47**, 561 (1993); J. Phys. G: Nucl. Part. Phys. **18**, 1533 (1992); S. S. Malik *et al.*, Pramana: J. Phys. **32**, 419 (1989); R. K. Puri *et al.*, Europhys. Lett. **9**, 767 (1989); J. Phys. G: Nucl. Part. Phys. **18**, 903 (1992).

[7] J. Blocki, J. Randrup, W. J. Świątecki, and C. F. Tsang, Ann. Phys. (NY) **105**, 427 (1977).

[8] W. Reisdorf, J. Phys. G: Nucl. Part. Phys. **20**, 1297 (1994).

[9] V. Y. Denisov, Phys. Lett. B **526**, 315 (2002).

[10] W. D. Myers and W. J. Świątecki, Phys. Rev. C **62**, 044610 (2000), and earlier references therein.

[11] M. Liu *et al.*, Nucl. Phys. A **768**, 80 (2006); A. Dobrowolski *et al.*, *ibid.* **729**, 713 (2003); J. Bartel *et al.*, Eur. Phys. J. A **14**, 179 (2002).

[12] V. Tripathi *et al.*, Phys. Rev. C **65**, 014614 (2001); S. Sinha, M. R. Pahlavani, R. Varma, R. K. Choudhury, B. K. Nayak, and A. Saxena, *ibid.* **64**, 024607 (2001); I. Padron *et al.*, *ibid.* **66**, 044608 (2002); J. O. Newton, R. D. Butt, M. Dasgupta, D. J. Hinde, I. I. Gontchar, C. R. Mortan, and K. Hagino, *ibid.* **70**, 024605 (2004); J. J. Kolata *et al.*, *ibid.* **69**, 047601 (2004); Z. H. Liu *et al.*, Eur. Phys. J. A **26**, 73 (2005); S. Mitsuoka, H. Ikezoe, K. Nishio, K. Tsuruta, S. C. Jeong, and Y. Watanabe, Phys. Rev. Lett. **99**, 182701 (2007); A. M. Stefanini *et al.*, Phys. Rev. C **78**, 044607 (2008); K. Washiyama and D. Lacroix, *ibid.* **78**, 024610 (2008); A. M. Stefanini *et al.*, Phys. Lett. B **679**, 95 (2009).

[13] R. Bass, Phys. Lett. B **47**, 139 (1973); Nucl. Phys. A **231**, 45 (1974).

[14] C. Ngô *et al.*, Nucl. Phys. A **252**, 237 (1975).

[15] S. K. Gupta and S. Kailas, Phys. Rev. C **26**, 747 (1982).

[16] N. G. Nicolis, Eur. Phys. J. A **21**, 265 (2004).

[17] R. Moustabchir and G. Royer, Nucl. Phys. A **683**, 266 (2001).

[18] W. D. Myers and W. J. Świątecki, Nucl. Phys. **81**(2), 1 (1966).

[19] W. D. Myers and W. J. Świątecki, Ark. Fys. **36**, 343 (1967).

[20] P. Möller and J. R. Nix, Nucl. Phys. A **361**, 117 (1981).

[21] P. Möller, J. R. Nix, W. D. Myers, and W. J. Świątecki, At. Data Nucl. Data Tables **59**, 185 (1995).

[22] W. D. Myers and W. J. Świątecki, Ann. Phys. (NY) **55**, 395 (1969); **84**, 186 (1974); Nucl. Phys. A **336**, 267 (1980).
[23] C. W. de Jager, H. de Vries, and C. de Vries, At. Data Nucl. Data Tables **14**, 479 (1974); H. de Vries, C. W. de Jager, and C. de Vries, *ibid.* **36**, 495 (1987).
[24] B. Nerlo-Pomorska and K. Pomorski, Z. Phys. A **348**, 169 (1994).
[25] V. Y. Denisov and N. A. Pilipenko, Phys. Rev. C **76**, 014602 (2007); A. S. Umar and V. E. Oberacker, *ibid.* **77**, 064605 (2008); M. Ismail, W. M. Seif, and M. M. Botros, Nucl. Phys. A **828**, 333 (2009).
[26] R. M. Anjos *et al.*, Phys. Lett. B **534**, 45 (2002).
[27] R. A. Broglia and A. Winther, *Heavy-Ion Reactions Lecture Notes* (Addison-Wesley, Redwood City, CA, 1981), p. 116.
[28] D. G. Kovar *et al.*, Phys. Rev. C **20**, 1305 (1979).
[29] P. R. Christensen and A. Winther, Phys. Lett. B **65**, 19 (1976).
[30] C. Ngô *et al.*, Nucl. Phys. A **240**, 353 (1975); F. Stancu *et al.*, *ibid.* **270**, 236 (1976); M. Ismail and M. M. Osman, Phys. Rev. C **24**, 458 (1981).
[31] H. Ngô and Ch. Ngô, Nucl. Phys. A **348**, 140 (1980).
[32] I. Dutt and R. K. Puri, Phys. Rev. C **81**, 044615 (2010).
[33] A. Winther, Nucl. Phys. A **594**, 203 (1995).
[34] I. Dutt and R. K. Puri Phys. Rev. C **81**, 064609 (2010).